HHS Public Access

Author manuscript

Nanomedicine. Author manuscript; available in PMC 2019 February 01.

Published in final edited form as:

Nanomedicine. 2018 February ; 14(2): 373–384. doi:10.1016/j.nano.2017.11.010.

Chemo-biologic combinatorial drug delivery using folate receptor-targeted dendrimer nanoparticles for lung cancer treatment

Narsireddy Amreddy, PhD[1,4], **Anish Babu, PhD**[1,4], **Janani Panneerselvam, PhD**[1,4], **Akhil Srivastava, PhD**[1,4], **Ranganayaki Muralidharan, MS**[1,4], **Allshine Chen, MS**[2], **Yan D. Zhao, PhD**[2,4], **Anupama Munshi, PhD**[3,4], and **Rajagopal Ramesh, PhD**[1,4,5,*]

[1]Department of Pathology, University of Oklahoma Health Sciences Center, Oklahoma City, OK, USA

[2]Department of Biostatistics and Epidemiology, University of Oklahoma Health Sciences Center, Oklahoma City, OK, USA

[3]Department of Radiation Oncology, University of Oklahoma Health Sciences Center, Oklahoma City, OK, USA

[4]Stephenson Cancer Center, University of Oklahoma Health Sciences Center, Oklahoma City, OK, USA

[5]Graduate Program in Biomedical Sciences, University of Oklahoma Health Sciences Center, Oklahoma City, OK, USA

Abstract

Co-administration of functionally distinct anti-cancer agents has emerged as an efficient strategy in lung cancer treatment. However, a specially designed drug delivery system is required to co-encapsulate functionally different agents, such as a combination of siRNA and chemotherapy, for targeted delivery. We developed a folic acid (FA) -conjugated polyamidoamine dendrimer (Den) -based nanoparticle (NP) system for co-delivery of siRNA against HuR mRNA (HuR siRNA) and *cis*-diamine platinum (CDDP) to folate receptor-α (FRA) -overexpressing H1299 lung cancer cells. The co-delivery of HuR siRNA and CDDP using the FRA-targeted NP had a significantly greater therapeutic effect than did individual therapeutics. Further, the FRA-targeted NP exhibited

*Corresponding Author: Rajagopal Ramesh, Department of Pathology, University of Oklahoma Health Sciences Center, Stanton L. Young Biomedical Research Center, Suite 1403, 975 N.E., 10th Street, Oklahoma City, OK 73104, USA; Phone: (405) 271-6101; rajagopal-ramesh@ouhsc.edu.

Author contributions

NA, **AB**, **JP, AS**, and **RM** – conducted the studies and collected data; **AC** and **YDZ** – performed statistical analysis; **NA**, **AB**, **JP, AS, RM**, **AC**, **YDZ**, **AM**, and **RR** - conceived and designed the studies; **NA** and **RR** wrote the manuscript. **NA**, **AB**, **JP, AS, RM**, **AC**, **YDZ**, **AM**, and **RR** -critically analyzed and interpreted the data; **NA**, **AB**, **JP, AS, RM**, **AC**, **YDZ**, **AM**, and **RR** - critically reviewed, provided suggestions and edited the manuscript; **RR** - supervised the project.

Conflict of Interest Disclosure

The authors report no conflicts of interest in this work.

improved cytotoxicity compared to non-targeted NP against lung cancer cells. Finally, the NP showed negligible toxicity towards normal MRC9 lung fibroblast cells. Thus, the present study demonstrates FRA-targeted Den nanoparticle system as a suitable carrier for targeted co-delivery of siRNA and chemotherapy agents in lung cancer cells.

Graphical Abstract

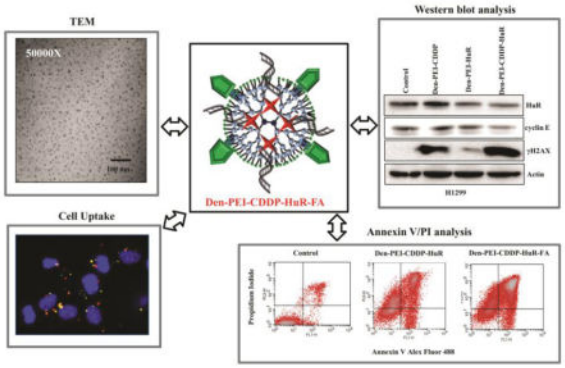

A novel chemotherapeutic (CDDP)-siRNA (HuR) combination was tested for its anti-tumor efficiency in lung cancer cells using folic acid conjugated Dendrimer-Polyethlyeneimine (Den-PEI) nanoparticles. This Den-PEI-CDDP-HuR-FA system showed favorable properties for targeted delivery and enhanced cell uptake in folate receptor alpha (FRA) overexpressing lung cancer cells. The targeted nanoparticle delivery also induced apoptosis, and demonstrated efficient combined therapeutic activity of CDDP and HuR siRNA in lung cancer cells.

Keywords

Lung cancer; dendrimer; FRA; CDDP; HuR siRNA

Background

The combined delivery of multiple chemotherapeutic agents to avoid the dose-dependent side effects of individual drugs has been effective, to some extent[1,2]. However, nonspecific drug delivery and reduced therapeutic effects due to poor bioavailability are unresolved issues[3]. Therefore, new delivery strategies are urgently needed to overcome these challenges.

Cis-diamminedichloroplatinum II (CDDP) is a platinum-based anti-cancer drug that is commonly used for the treatment of lung cancer[4,5]. CDDP intercalates into the cellular DNA forming DNA adducts resulting in apoptosis[6]. A major limitation of CDDP is its ability to form DNA adducts in normal tissue resulting in non-specific toxicity; hence, a tumor-targeted carrier is required for improve therapeutic efficacy while minimizing non-specific toxicity [7–9]. Studies have shown co-delivery of CDDP and tumor suppressor genes enhances the therapeutic efficacy[10].

We and others reported that human antigen R (HuR), an RNA-binding protein that influences the translation of key survival and growth-related mRNAs in cancer cells, is a potential cancer therapy target[11,12]. HuR is elevated in lung cancer compared with normal healthy cells[13, 14]. Overexpression of HuR is implicated in tumorigenesis[15], cancer cell immune recognition, and metastasis[16–18]. Reports suggest that HuR gene downregulation suppresses tumor growth and metastasis[19]. RNAi-based gene silencing methods, especially the use of small interfering RNA (siRNA), hold great promise for efficient HuR downregulation[20, 21]. Based on these reports we hypothesized that combining HuR siRNA and CDDP would improve the therapeutic index of these individual agents against lung cancer.

Metallic and polymer-based nanocarrier delivery systems have garnered considerable attention as anti-cancer drug carriers[22–24]. Among those drug delivery systems, poly (amidoamine) (PAMAM) dendrimers has advantages, such as the availability of numerous free amino groups that can be functionalized with multiple biomolecules and the ability to incorporate hydrophilic and/or hydrophobic drugs[25–27]. Moreover, dendrimers functionalized with targeting ligands can effectively deliver chemotherapeutics and siRNA specifically into tumor tissues[28,29]. Various surface receptors, among which folate receptor alpha (FRA) is well-recognized for targeted drug delivery, are overexpressed in lung cancer cells[30].

In the present work, we designed a PAMAM dendrimer-based nanoparticle system for FRA-targeted delivery of a combination of HuR siRNA and CDDP and tested its efficacy using lung cancer cells as a model.

Methods

Preparation of Den-PEI-CDDP-siRNA-FA nanoparticles

In the first step of Den-PEI-CDDP-siRNA-FA nanoparticle preparation, polyethyleneimine (PEI) was covalently conjugated to fourth-generation (G4, 64 amine surface groups) Poly (amidoamine) dendrimer (Den) through a bifunctionalized PEG crosslinker molecule. Briefly, 1:10 molar ratios of 1.4 μmol Den (20mg) and 14 μmol PEI (11.8μg) were dissolved in 2 ml of Tris-HCl (pH 7.4). To this mixture, 14 μmols of the NHS-PEG-NHS (28μg) cross-linker was added to conjugate the surface amine groups of dendrimer with PEI amine groups. Then, the reaction mixture was stirred at room temperature (RT) for 24 h, followed by purification by dialysis against Tris-HCl (pH 7.4; 8 KDa MW cutoff membrane) to remove the unbound molecules. The resulting Den-PEI nanoparticles were used in subsequent steps as described below.

CDDP encapsulation into Den-PEI nanoparticles was carried out *via* hydrolysis[31]. Briefly, 15 mg of CDDP was dissolved in 10 ml of de-ionized water with vigorous stirring at RT, followed by the addition of 20 mg of Den-PEI nanoparticles and stirring continued at RT in the dark for 24 h. After completing the reaction, unbound CDDP was removed by dialyzing Den-PEI-CDDP complex against Tris-HCl. To calculate the CDDP encapsulation efficiency, we measured the unbound CDDP concentration and compared it with the known CDDP concentrations standard curve using a colorimetric O-phenylenediamine (OPDA) assay, as

mentioned in the supplementary material. The FA-PEG-NHS was conjugated to Den-PEI-CDDP (Den-PEI-CDDP-FA) through amide covalent linkage; the detailed procedure is mentioned in the supplementary material.

Next, siRNA was encapsulated via electrostatic interaction in Den-PEI-CDDP and Den-PEI-CDDP-FA nanoparticles by mixing the nanoparticles with siRNA (N/P ratio 10) in Tris-HCl (pH 7.4) buffer and incubating at RT for 20 min. The formation of the Den-PEI-CDDP-siRNA and Den-PEI-CDDP-siRNA-FA nanoparticles was confirmed with agarose gel. The protection of siRNA in the Den-PEI-CDDP-siRNA nanoparticle complex was studied using an agarose gel retardation assay. Briefly, Den-PEI-CDDP-siRNA nanoparticles were incubated in 10% fetal bovine serum (FBS) Tris-HCl (pH 7.4) buffer at 37°C. After 30 min, 1 h, and 3 h of incubation, aliquots from each sample were collected. Then, the siRNA protection was confirmed by agarose gel, as mentioned in the supplementary material.

Cell lines

Non-small-cell lung cancer (H1299 and A549) and normal lung fibroblast (MRC9) cell lines were maintained in RPMI-1640 and MEM medium respectively, and cultured as described previously [32].

In vitro cellular uptake of Den-PEI-CDDP-siGLO nanoparticles

Cell uptake of the Den-PEI-CDDP-siGLO nanoparticles was studied by measuring fluorescence intensity (FI) and fluorescence microscopy images in H1299 cells using fluorescent siRNA (siGLO, red). For cell uptake measurements, H1299 cells were seeded in 6-well plates or on coverslips, and treated with Den-PEI-CDDP-siGLO nanoparticles with 50 and 100 nM of siGLO concentrations per well. Untreated groups served as controls. After 24 h, cells were harvested and washed with PBS. The fluorescence was measured with an Envision multiplate reader (Perkin Elmer, Santa Clara, CA, USA) with excitation 555 nm and emission 570 nm wavelengths. The obtained fluorescence intensity was normalized to 10000 cells. Cells seeded on coverslips were stained using LysoTracker® green (7.5 μl) per the manufacturer's protocol (Thermo Fisher, LysoTracker® Green DND-26) for 2 h. Then, the coverslips were processed for microscopy images, as described earlier [33]. Fluorescence images of cells were acquired using a Nikon TiU microscope attached to a charge-coupled device (CCD) camera (Nikon Instruments, Inc., New York, NY, USA) and imported into ImageJ analysis software (NIH, Bethesda, MD, USA).

Next, we studied the role of receptor-mediated endocytosis in cell uptake of FRA-targeted nanoparticles through a temperature dependency assay and a receptor blocking study in the presence of exogenous folic acid-containing media. For the temperature-dependent uptake study, H1299 cells were grown in 6-well plates and then added to the Den-PEI-CDDP-siGLO or Den-PEI-CDDP-siGLO-FA formulations with equivalent siGLO concentrations (50 nM). The plates were then kept either at 37 °C or 4 °C for 4 h. The cells were then harvested. The siGLO-fluorescence was measured and compared with the fluorescence obtained from non-FA-targeted Den-PEI-CDDP-siGLO nanoparticle-treated cells.

In the folate receptor blocking study, H1299 cells were incubated with one of the following media: regular RPMI-1640 medium, in which a minimum amount of folic acid is present,

folic acid-free RPMI-1640 medium, or RPMI-1640 medium with 1 mM of exogenous folic acid added. After 24 h of incubation, 1 h of serum starvation was carried out. We added Den-PEI-siGLO-FA nanoparticles containing 50 nM siGLO and incubated them for 24 h. The cells were then collected and the siGLO fluorescence was measured as mentioned above.

Cell viability assay

Cell viability assays were conducted using the standard trypan blue exclusion assay[33]. In a typical cell viability experiment, H1299 and A549 (0.1×10^6) cells were grown in 6-well plates and were treated with Den-PEI-CSi (scrambled siRNA) or Den-PEI-HuR (HuR siRNA) for 72 h with 100 nM of siRNA per well. Untreated cells served as controls.

In a separate study, we tested the cytotoxicity of Den-PEI-CDDP, Den-PEI-HuR, and Den-PEI-CDDP-HuR with equivalent concentrations of CDDP (10 μM) and HuR siRNA (100 nM) in H1299, A549, and MRC9 cells. Cells that received no treatment served as controls.

For determining the cell killing efficiencies between targeted and non-targeted nanoparticles, cells were treated with Den-PEI-HuR-FA and compared against Den-PEI-HuR and Den-PEI-CDDP-HuR-treated cells were compared to Den-PEI-CDDP-HuR-FA-treated cells.

Western blot assay

Total cell lysates prepared from cells receiving different treatments were analyzed for HuR, cyclin E (1:1,000 dilution; Santa Cruz Biotechnology, Dallas, TX, USA), caspase9, PARP, and γH2AX (1:500; Cell Signaling Technology, Inc., Danvers, MA, USA) by western blot analysis as previously described[13]. Actin (1:2,000; Sigma Chemicals, St Louis, MO, USA) was used as an internal loading control. The relative protein expression compared to beta-actin was quantified using GelQuant software (Syngene) as previously described[13,14].

Apoptotic Analysis

Apoptotic cell death was determined using the Alexa Fluor-488-Annexin V/Propidium Iodide (PI) (Thermo Fisher Scientific, Eugene, OR USA) staining kit per the manufacturer's protocol. Briefly, H1299 cells grown in 6-well plates were treated with Den-PEI-CDDP-HuR and Den-PEI-CDDP-HuR-FA for 72 h (10 μM CDDP and 100 nM HuR per well). Untreated cells served as controls. The treated cells were harvested and washed with PBS. Then, the cells were stained with 5 μl of Alexa Fluor-488-Annexin V and 1 μl of PI (1mg/ml) solution for 15 min at room temperature. The percent of cells undergoing apoptotic death was measured with a FACS Calibur flow cytometer using the Cell Quest software (BD Biosciences). The percentage of apoptotic cells was calculated as the percentage sum of Annexin-V-positive (Q2) and Annexin-V/PI-positive (Q3) cell population.

Supplementary Materials

Further detailed materials and methods, characterization and optimization of FA and CDDP, and results are given in the supplementary materials.

Statistics

Each experiment was repeated at least three separate times (n=3) and the data are represented as mean ± standard deviation. Response variables, including percent cell viability, fluorescence, HuR mRNA, and western blot quantifications, were compared among treatment groups using one-way analysis of variance. A *P*-value less than 0.05 were considered statistically significant. SAS 9.2 software (SAS Institute Inc., Cary, NC) was used for the statistical analysis.

Results

Synthesis and characterization of Den-PEI-CDDP-HuR-FA nanoparticles

The fourth-generation Poly (amidoamine) dendrimer nanoparticles (G4-PAMAM) were modified with FA for the co-delivery of HuR siRNA and CDDP specifically towards FRA-overexpressing lung cancer cells. The G4-PAMAM dendrimer contains peripheral amine groups, of which 10% were exploited for modification using PEI. The scheme of Den-PEI-CDDP-HuR-FA synthesis is shown in Supplementary Figure 1. Low molecular weight (800 MW), branched PEI was covalently conjugated by using an NHS-PEG-NHS crosslinker that enhances the net positive charge of the particle to absorb negatively charged siRNA electro-statistically with high efficiency. Addition of PEI improves the endosomal escape and transfection efficiency of siRNA[34]. The PEI modification was confirmed by zeta potential measurements.

Bare dendrimer nanoparticles showed an average charge of +5.9 mV (Figure 1A). After conjugating with PEI, the charge increased to +8.75 mV and is likely due to the enormous amine groups of PEIs. Determination of the size and shape of the Den-PEI nanoparticles by TEM imaging showed well-dispersed spherical particles less than 10 nm in size. (Figure 1B).

Dendrimers possess several primary and secondary amine groups that contribute in forming complexes between CDDP and PAMAM dendrimers through coordinate bonds[35]. The encapsulation efficiencies for CDDP were 35.65 ± 5.65 and 40.52 ± 4.18% in Den-PEI and Den-PEI-FA nanoparticles respectively (Table 1). This result shows that folic acid conjugation did not markedly alter the CDDP encapsulation efficiency. The encapsulation of CDDP by Den-PEI (Den-PEI-CDDP) nanoparticles increased its zeta potential from +8.75 mV to +14.5 mV (Figure 1A). To target FRA receptors, the surface amine groups of the Den-PEI-CDDP nanoparticles were covalently conjugated with pre-synthesized folic acid-PEG-NHS linker through an amide bond. The presence of folic acid in Den-PEI-CDDP-FA nanoparticles was confirmed by an absorption maximum of 280 nm, as evidenced by increases in peak intensity with increasing folic acid concentrations (Supplementary Figure 2). The addition of FA to Den-PEI-CDDP increased the zeta potential from +14.5 mV to +17.2 mV.

The dendrimer nanoparticles showed positive surface charges when dispersed in Tris-HCl pH 7.4 buffer, which allows the complexation of Den with negatively charged siRNA[36]. The Den-PEI-CDDP and Den-PEI-CDDP-FA nanoparticles were complexed with siRNA through electrostatic interaction at an N/P ratio of 10. The zeta potential of Den-PEI-CDDP

(+14.5mV) was reduced upon siRNA complexation (+5.1mV). siRNA complexation reduced the zeta potential of Den-PEI-CDDP-FA nanoparticles from +17.2 mV to +6.07 mV, due to the negative charge contribution from siRNA (Figure 1A). Determination of siRNA encapsulation efficiency showed 97.84 ± 0.12 and 97.87 ± 0.10 % of siRNA was encapsulated in Den-PEI and Den-PEI-FA nanoparticles respectively (Table 1). Again our study results demonstrated that folic acid conjugation produced negligible change in the siRNA encapsulation of nanoparticles. TEM images of Den-PEI-CDDP-siRNA-FA nanoparticles represent the conjugations of CDDP, siRNA, and FA that did not affect nanoparticle size, compared with Den-PEI (Figure 1B, C).

The siRNA encapsulation in the Den-PEI-CDDP-siRNA and Den-PEI-CDDP-siRNA-FA nanoparticles was confirmed with an agarose gel electrophoretogram (Figure 2A). The siRNA contained the nanoparticles remained in the wells (as evidenced by ethidium bromide glowing in the wells), whereas free siRNA moved into the gel as a result of electrophoresis. These data confirmed the complexation of siRNA with Den-PEI-CDDP and Den-PEI-CDDP-FA nanoparticles. Apart from encapsulation, Den-PEI-CDDP nanoparticles protected the siRNA from degradation in the presence of serum (10% FBS) even after 3 h of incubation, as the complex incubated with serum remained in the wells, without causing any smear in the gel (Figure 2B). The lack of visible leaching of siRNA into the gel during electrophoresis indicates complete protection of siRNA by the Den-PEI-CDDP nanoparticles.

CDDP and siRNA release kinetics from Den-PEI-CDDP-siRNA and Den-PEI-CDDP-siRNA-FA nanoparticles

The CDDP and siRNA release profiles from Den-PEI-CDDP-siRNA nanoparticles were carried out in serum-free medium and in medium with 10% FBS containing Tris-HCl buffer (pH 7.4). The CDDP release was higher and faster in the presence of serum (34%) compared to 26% in the absence of serum at 7 h (Figure 2C). The CDDP release pattern from Den-PEI-CDDP-siRNA-FA (28%) and Den-PEI-CDDP-siRNA (26%) nanoparticles were similar indicating that folic acid conjugation has no influence on CDDP release profile.

SiRNA release study showed Den-PEI-CDDP-siRNA had released 28% and 20% of siRNA in the absence and presence (10%) of FBS respectively at 24 h (Figure 2D). The lower siRNA release in 10% FBS-containing buffer may be attributable to siRNA degradation, which might have influenced the low level of detection at 24 h by the PicoGreen assay[37]. After folic acid conjugation, 34% of siRNA was released from Den-PEI-CDDP-siRNA-FA. This finding also indicates that the folic acid conjugation does not influence the siRNA release profile. Our results demonstrate that CDDP and siRNA have distinct release patterns from Den-PEI-CDDP-siRNA and Den-PEI-CDDP-siRNA-FA nanoparticles *in vitro* and do not influence each other.

Cell uptake and endosomal escape of Den-PEI-CDDP-siGLO nanoparticles

Cell uptake studies were carried out in H1299 cells with Den-PEI-CDDP nanoparticles encapsulated with 50 nM or 100 nM concentrations of siGLO siRNA. A dose-dependent increase in fluorescence intensity was observed at 24 h post Den-PEI-CDDP-siGLO

treatment. A 3-fold enhancement in fluorescence intensity (FI; average 11395 a.u., $p < 0.01$) was observed when cells were incubated with 50 nM siGLO siRNA contained in Den-PEI-CDDP compared with the untreated control group (4081 a.u.; Figure 3A). The FI was further increased (average 17590 a.u., $p < 0.01$) when siGLO concentration increased to 100 nM. Fluorescence microscopy images (Figure 3B) showed punctate red fluorescence in the cytoplasm of Den-PEI-CDDP-siGLO-treated cells that concurred with the FI study results. Further, our studies showed majority of the siGLO siRNA-contained in the nanoparticles escaped the lysosomes/endosomes compartment and entered the cytoplasm (red fluorescence) with some still trapped in the endosome/lysosomes (orange fluorescence) as evidenced by the LysoTracker Green staining (Figure 3B). These results indicate that Den-PEI-CDDP-siGLO nanoparticles are efficiently taken up by the cells and the Den-PEI nanoparticles allow the escape of siRNA from endosome/lysosomes into the cytoplasm.

Nanoparticle uptake occurs via cell receptor-mediated endocytosis

The optimal FA concentration was measured as 3.75 μg/ml of FA-PEG-NHS on Den-PEI nanoparticles in H1299 cells, based on FI of siGLO (Supplementary Figure 3A). Then, the specific receptor-mediated cell uptake study was confirmed by two different methods. At lower temperatures, cell surface receptors are generally inactive. Thus, the low temperature hinders the receptor-mediated uptake of nanoparticles. In the present study, temperature-dependent receptor-mediated uptake studies were carried out in H1299 cells after incubation with Den-PEI-CDDP-siGLO-FA nanoparticles for 4 h at either 37 °C or 4 °C. Den-PEI-CDDP-siGLO-FA nanoparticles showed the highest fluorescence intensity (average 12531 a.u.; $p < 0.01$) compared with Den-PEI-CDDP-siGLO (average 7851 a.u.; $p < 0.01$) and untreated controls (average 1408 a.u.) at 37 °C (Figure 4A). However, at 4 °C the Den-PEI-CDDP-siGLO-FA (average 3746 a.u.) showed decreased fluorescence intensity in cell uptake compared with the Den-PEI-CDDP-siGLO (3968 a.u.) nanoparticles. The results clearly demonstrate the specific receptor-mediated uptake tendency of the Den-PEI-CDDP-siGLO-FA nanoparticles.

Den-PEI-siGLO-FA uptake was further confirmed by a folate receptor blocking study with the addition of exogenous folic acid (1mM) in the medium prior to Den-PEI-siGLO-FA treatment. The FRA blocking study was performed in H1299 cells with three different FA concentrations in RPMI-1640 medium (Figure 4B). The highest fluorescence intensity was observed with FA-free RPMI-1640 medium (average 8455 a.u.; $p < 0.01$), followed by regular RPMI-1640 medium (average 6452 a.u.), and RPMI-1640 medium with 1 mM excess FA added (3985 a.u.). This finding demonstrates that Den-PEI-siGLO-FA nanoparticle uptake by FRA-overexpressing cells depended on FA concentration in the medium; with increasing FA concentrations, the uptake of Den-PEI-FA-siGLO nanoparticles decreased. Further, Den-PEI-siGLO-FA nanoparticle uptake by cells occurs via folate receptor-mediated endocytosis

Den-PEI-based CDDP and HuR siRNA co-delivery enhances the therapeutic efficiency in lung cancer cells, while sparing normal cells

Treatment with Den-PEI-CDDP and Den-PEI-HuR resulted in approximately 29% and 23% growth inhibition in H1299 cells at 72 h (Figure 5A). When the CDDP and HuR siRNA

were combined with Den-PEI-CDDP-HuR nanoparticles, cell growth inhibition was significantly enhanced to 50% (p <0.01). In A549 cells, Den-PEI-CDDP and Den-PEI-HuR produced approximately 34% and 30% growth inhibition respectively. Strikingly, Den-PEI-CDDP-HuR nanoparticles treatment produced 62% growth inhibition (p <0.01; Figure 5A). In contrast, both Den-PEI-CDDP and Den-PEI-HuR nanoparticles treatment showed 18% growth inhibition in normal MRC9 lung fibroblast cells. When MRC9 cells were treated with Den-PEI-CDDP-HuR nanoparticles, the growth inhibition (27%; p=NS) was comparable to that of individual treatments using Den-PEI-CDDP or Den-PEI-HuR nanoparticles.

The combined therapeutic efficacy of Den-PEI-CDDP-HuR was further evaluated through western blot analysis. Irrespective of formulation, HuR siRNA significantly induced HuR knockdown in H1299 and A549 cancer cells (Figure 5B & C). Associated with HuR knockdown was the marked reduction in HuR-regulated cyclin E levels for Den-PEI-HuR and Den-PEI-CDDP-HuR nanoparticle treatments. In parallel, significant induction of γH2AX expression which is a marker for DNA damage was observed in both H1299 and A549 cells treated with Den-PEI-CDDP and Den-PEI-CDDP-HuR nanoparticles compared with Den-PEI-HuR and untreated control cells (Figure 5B & C). Further, γH2AX expression was higher (p<0.01) in Den-PEI-CDDP-HuR nanoparticle treatment compared to Den-PEI-CDDP nanoparticle suggesting CDDP and HuR siRNA combination produced increased DNA damage.

In MRC9 cells, Den-PEI-HuR treatment albeit produced some reduction in HuR (Figure 5B; p<0.05) when compared to untreated control, the difference in HuR knockdown was negligible when compared to Den-PEI-CDDP. HuR knockdown however was significant with Den-PEI-CDDP-HuR treatment compared to all other treatments (p<0.01). Cyclin E also showed a slight reduction of expression Den-PEI-CDDP-HuR treatment correlating with HuR knockdown effects. Examination for γH2AX expression showed modest increase after treatment with Den-PEI-HuR and Den-PEI-CDDP-HuR nanoparticles (p<0.01). Surprisingly, reduction in γH2AX expression was observed in Den-PEI-CDDP nanoparticles treated cells compared to untreated control. Therefore, it appears that Den-PEI-CDDP-HuR nanoparticles controlled and reduced the cytotoxic effect on normal cells while imparting therapeutic efficiency in cancer cells.

We also verified the effect in the HuR mRNA knockdown using qRT-PCR analysis. Significant reductions in HuR mRNA levels was observed in Den-PEI-HuR- (~70%) and Den-PEI-CDDP-HuR (~55%) nanoparticles-treated H1299 cells at 72 h, compared with untreated control and Den-PEI-CDDP nanoparticles (Figure 6; p <0.01). In A549 cells, Den-PEI-HuR and Den-PEI-CDDP-HuR nanoparticle treatment reduced the mRNA levels about 65% and 66% respectively (p <0.01). In MRC9 cells, Den-PEI-HuR- and Den-PEI-CDDP-HuR- treatment reduced HuR mRNA levels by 64% and 32% respectively when compared to untreated control cells. Interestingly, the reduction in HuR mRNA did not correlate with HuR protein levels in Den-PEI-CDDP-HuR- and Den-PEI-HuR-treated MRC9 cells. The underlying cause for the difference in correlation between HuR mRNA and protein in MRC9 cells is not clear but could be speculated to be due to differences in post-translational

regulation and processing in normal versus tumor cells[38]. Furthermore, the observation made in the present study is not unique and concurs with our recent report support[39].

In A549 and MRC9 but not in H1299 cells, Den-PEI-CDDP treatment did reduce HuR mRNA compared to control. These results indicated further improvements are needed to increase tumor cell cytotoxicity and spare normal cells. Hence, we next tested FRA-targeted nanoparticle (Den-PEI-CDDP-HuR-FA), for enhanced therapeutic efficiency in FRA-overexpressing lung cancer cells.

FRA-targeted siHuR specific delivery into H1299 cells

We have previously reported H1299 cells overexpress of FRA[40]. Thus, these cells are a suitable tumor cell model with which to demonstrate the targeted delivery efficiency of Den-PEI-HuR-FA nanoparticles in comparison with non-targeted nanoparticles. As shown in Figure 7A, Den-PEI-HuR-FA nanoparticle treatment produced 33% growth inhibition compared to 21% inhibition produced by Den-PEI-HuR nanoparticle treatment (p <0.01) over untreated control at 72 h. Correlating with the growth inhibitory activity, significant reduction in HuR and cyclin E protein levels were observed in both, Den-PEI-HuR-FA- and Den-PEI-HuR- nanoparticle treated cells compared to untreated control (Figure 7B & C; p<0.01). However, the reduction in these proteins was greater in cells treated with Den-PEI-HuR-FA nanoparticles than in cells treated with Den-PEI-HuR nanoparticles. These results demonstrate that FRA-targeted Den-PEI-HuR-FA nanoparticles are more efficient in enhancing the therapeutic efficacy of HuR siRNA in a FA expressing lung cancer cell line.

Den-PEI-CDDP-HuR-FA nanoparticles efficiently delivered and enhanced therapeutic efficiency in FRA-overexpressing H1299 cells

Since Den-PEI-HuR-FA nanoparticles showed greater growth inhibition, we next investigated whether enhanced antitumor activity could be also observed when CDDP is incorporated in the Den-PEI-HuR-FA nanoparticle formulation. Both Den-PEI-CDDP-HuR-FA and Den-PEI-CDDP-HuR nanoparticle treatment produced significant cell growth inhibition compared to untreated control at 72 h (Figure 8A; p<0.01). However, Den-PEI-CDDP-HuR-FA nanoparticle treatment produced greater growth inhibitory activity (~64%; p<0.01) compared to Den-PEI-CDDP-HuR nanoparticle treatment (~50%; p <0.01).

The protein expression analysis showed a strong correlation with the growth inhibition results. Compared with Den-PEI-CDDP-HuR nanoparticles, the Den-PEI-CDDP-HuR-FA nanoparticles significantly reduced HuR and cyclin E protein expression while concomitantly increasing caspase 9 and PARP cleavage, which are markers indicative of cells undergoing apoptosis (Figure 8B & C; p <0.01). Further evidence for cells undergoing apoptosis was revealed by Annexin V staining. As shown in Figure 8D, Den-PEI-CDDP-HuR-FA nanoparticle treatment (~71% apoptotic cells) showed 25% and 32% (p <0.01) higher apoptosis than did Den-PEI-CDDP-HuR nanoparticles (~45% apoptotic cells) and positive control free CDDP (~38% apoptotic cells), respectively. Finally, γH2AX was also significantly expressed with Den-PEI-CDDP-HuR-FA nanoparticles compared with Den-PEI-CDDP-HuR nanoparticles (Figure 8B& C; p <0.01). These findings demonstrate that combined delivery of CDDP and HuRsiRNA to FRA-overexpressing lung cancer cells can

be achieved using the FA-targeted Den-PEI delivery system to produce increased antitumor activity while reducing the cytotoxicity to normal cells.

Discussion

In the present study, we developed and evaluated a nanoparticle system based on a PAMAM-dendrimer-PEI conjugate for the co-delivery of HuR siRNA and CDDP for cancer therapy. Incorporation of PEI via conjugation to the dendrimer improved the siRNA complexation and endosomal escape efficiency[41]. Further, the use of a PEG linker between the PEI and dendrimer molecules improved the dispersibility of the complex in aqueous solution. Using two different methods we successfully encapsulated CDDP and HuR siRNA in the nanoparticle. The primary and secondary amine groups of PAMAM dendrimers contribute to the formation of coordinate bonds with the platinum of CDDP through hydrolysis that resulted in a CDDP encapsulation efficiency of 35.65%. The protonated Tris-HCl (pH 7.4) buffer increases the positive surface charge of amine groups, while converting amine groups to amino groups that facilitated the siRNA complexation with the dendrimer by electrostatic adsorption in Tris-HCl pH 7.4 buffer[32] as illustrated in Supplementary Figure 1. The resulting nanoparticles had favorable physicochemical properties, such as particle size, zeta potential, drug and siRNA encapsulation efficiencies, and *in vitro* release profiles, indicating that the nanoparticle system will be efficient in delivering a combination of siRNA and CDDP to lung cancer cells.

Although our nanoparticles exhibited favorable physicochemical properties, there are numerous barriers that need to be overcome for achieving significant and measurable therapeutic efficacy. The first barrier is the issue of siRNA stability in particular under *in vivo* conditions. The presence of serum proteins in particular often destabilizes siRNA and allows for rapid bio-clearance before reaching its target. Another barrier that restricts nucleic acids and siRNA efficacy is the endosome compartment that traps and degrades them thus reducing their entry into the cytoplasm. Thus, for having successful cancer treatment outcomes the nanodrug delivery system should be able to overcome these barriers. In the present study, the Den-PEI nanoparticles not only protected the siRNA in the presence of serum but also showed that it facilitated the endo-lysosomal escape of siRNA and successfully induced silencing of the target gene in cancer cells. Another factor for consideration is the release rate kinetics when two different types of therapeutics such as siRNA and chemotherapy are used; here, simultaneous CDDP and HuR siRNA release occurred from dendrimer nanoparticles, initiating the therapeutic process. Finally, therapeutic efficacy against cancer cells needs to be achieved without having off-target effects and increasing untoward non-specific toxicity to normal cells. As shown in Supplementary Figure 4 A & B, although Den-PEI-HuR nanoparticles markedly suppressed HuR in lung cancer cells and inhibited their growth ($p<0.05$), some degree of cytotoxicity was also observed in Den-PEI-control (c) si treatment when compared to untreated control cells. This observation warranted development and testing of tumor-targeted nanoparticle delivery system. Further, it was realized that HuR knockdown alone was not sufficient to eliminate cancer completely; and that combining with other anti-cancer agents was needed. For this purpose we exploited the FA overexpression in lung cancer and tested FRA-targeted dendrimer nanoparticles for CDDP and HuRsiRNA combinatorial therapy.

CDDP as the drug of choice was selected because it is the front-line chemotherapeutic used to treat lung cancer. The rationale to select HuR as a molecular target for therapy is because it has been implicated in regulating key cellular processes by binding to mRNAs, and controls the expression of proteins involved in cancer cell growth, proliferation, and metastasis[18]. Further, specific knockdown of HuR using siRNA[39,42] or small molecule inhibitors[43–45] has been shown to downregulate cancer pathology-related proteins resulting in pronounced anticancer activity[19]. Herein, we demonstrated combination therapy using FRA-targeted dendrimer nanoparticles exhibited specificity and selectivity towards FRA overexpressing cancer cells that improved the therapeutic efficiency and also reduced the cytotoxicity towards normal cells. The combined therapeutic effect with HuR siRNA was observed at low CDDP concentrations (IC_{20} value). At higher concentrations of CDDP, the cellular toxicity was high (Supplementary Figure 3B) that masked the growth inhibitory effects of siRNA-based gene knockdown. Moreover, use of high CDDP concentrations would lead to undesirable toxicity in normal cells and thus making the nano-delivery approach non-translatable to the clinic[33]. Finally, molecular studies revealed FRA-targeted dendrimer nanoparticle therapy induced greater DNA damage and apoptotic cell death compared to non-targeted nanoparticle treatment. In conclusion our study results demonstrate combined delivery of CDDP and HuR siRNA is feasible using FRA-targeted dendrimer nanoparticle for treating FRA-overexpressing lung cancer cells, while minimizing their toxicity to normal cells. Our studies provide a platform for conducting advanced *in vivo* studies using lung tumor xenograft models.

Supplementary Material

Refer to Web version on PubMed Central for supplementary material.

Acknowledgments

Funding Support. The work was supported in part by a grant received from the National Institutes of Health (NIH), R01 CA167516 (RR), an Institutional Development Award (IDeA) from the National Institute of General Medical Sciences (P20 GM103639) of the National Institutes of Health (RR & AM), and by funds received from the Stephenson Cancer Center Seed Grant (RR), Presbyterian Health Foundation Seed Grant (RR), Presbyterian Health Foundation Bridge Grant (RR) and Jim and Christy Everest Endowed Chair in Cancer Developmental Therapeutics (RR) at the University of Oklahoma Health Sciences Center. Rajagopal Ramesh is an Oklahoma TSET Research Scholar and holds the Jim and Christy Everest Endowed Chair in Cancer Developmental Therapeutics.

The authors thank Ms. Kathy Kyler at the office of Vice President of Research, OUHSC, for editorial assistance.

Abbreviations

Den	polyamidoamine dendrimer
CDDP	Cis-diamminedichloroplatinum II
FA	folic acid
FRA	folate receptor-α
HuR	human antigen R

siRNA	small interfering RNA
PEI	polyethyleneimine
OPDA	O-phenylenediamine

References

1. Schild SE, Vokes EE. Pathways to improving combined modality therapy for stage III nonsmall-cell lung cancer. Ann Oncol. 2016; 27:590–9. [PubMed: 26712904]
2. Ren Z, Zhou S, Liu Z, Xu S. Randomized controlled trials of induction treatment and surgery versus combined chemotherapy and radiotherapy in stages IIIA-N2 NSCLC: a systematic review and meta-analysis. J Thorac Dis. 2015; 7:1414–22. [PubMed: 26380768]
3. Florea AM, Büsselberg D. Cisplatin as an anti-tumor drug: cellular mechanisms of activity, drug resistance and induced side effects. Cancers (Basel). 2011; 3:1351–71. [PubMed: 24212665]
4. Sears CR, Cooney SA, Chin-Sinex H, Mendonca MS, Turchi JJ. DNA damage response (DDR) pathway engagement in cisplatin radiosensitization of non-small cell lung cancer. DNA Repair (Amst). 2016; 40:35–46. [PubMed: 26991853]
5. Babu A, Amreddy N, Ramesh R. Nanoparticle-based cisplatin therapy for cancer. Ther Deliv. 2015; 6:115–9. [PubMed: 25690081]
6. Shi S, Tan P, Yan B, Gao R, Zhao J, Wang J, et al. ER stress and autophagy are involved in the apoptosis induced by cisplatin in human lung cancer cells. Oncol Rep. 2016; 35:2606–14. [PubMed: 26985651]
7. Wen J, Zeng M, Shu Y, Guo D, Sun Y, Guo Z, et al. Aging increases the susceptibility of cisplatin-induced nephrotoxicity. Age (Dordr). 2015; 37:112. [PubMed: 26534724]
8. Hu W, Jin P, Liu W. Periostin Contributes to Cisplatin Resistance in Human Non-Small Cell Lung Cancer A549 Cells via Activation of Stat3 and Akt and Upregulation of Survivin. Cell Physiol Biochem. 2016; 38:1199–208. [PubMed: 26982182]
9. Florea AM, Büsselberg D. Cisplatin as an anti-tumor drug: cellular mechanisms of activity, drug resistance and induced side effects. Cancers (Basel). 2011; 3:1351–71. [PubMed: 24212665]
10. Babu A, Wang Q, Muralidharan R, Shanker M, Munshi A, Ramesh R. Chitosan coated polylactic acid nanoparticle-mediated combinatorial delivery of cisplatin and siRNA/Plasmid DNA chemosensitizes cisplatin-resistant human ovarian cancer cells. Mol Pharm. 2014; 11:2720–33. [PubMed: 24922589]
11. Nabors LB, Gillespie GY, Harkins L, King PH. HuR, a RNA stability factor, is expressed in malignant brain tumors and binds to adenine- and uridine-rich elements within the 3′ untranslated regions of cytokine and angiogenic factor mRNA. Cancer Res. 2001; 61:2154–61. [PubMed: 11280780]
12. Lu S, Mott JL, Harrison-Findik DD. Saturated fatty acids induce post-transcriptional regulation of HAMP mRNA via AU-rich element-binding protein, human antigen R (HuR). J Biol Chem. 2015; 290:24178–89. [PubMed: 26304124]
13. Muralidharan R, Panneerselvam J, Chen A, Zhao YD, Munshi A, Ramesh R. HuR-targeted nanotherapy in combination with AMD3100 suppresses CXCR4 expression, cell growth, migration and invasion in lung cancer. Cancer Gene Ther. 2015; 22:581–90. [PubMed: 26494555]
14. Muralidharan, R., Babu, A., Basalingappa, K., Mehta, M., Munshi, A., Ramesh, R. Designing of tumor-targeted HuR siRNA nanoparticle as a therapeutic for lung cancer. In: Gandhi, V.Mehta, K.Grover, RK.Pathak, S., Aggarwal, BB., editors. Multitargeted Approach to the Treatment of Cancer. Springer International Publishing; Switzerland: 2015. p. 277-94.
15. Wang J, Wang B, Bi J, Zhang C. Cytoplasmic HuR expression correlates with angiogenesis, lymphangiogenesis, and poor outcome in lung cancer. Med Oncol. 2011; 28(Suppl1):S577–85. [PubMed: 21046284]
16. Moradi F, Berglund P, Linnskog R, Leandersson K, Andersson T, Prasad CP. Dual mechanisms of action of the RNA-binding protein human antigen R explains its regulatory effect on melanoma cell migration. Transl Res. 2016; 172:45–60. [PubMed: 26970271]

17. Chai Y, Liu J, Zhang Z, Liu L. HuR-regulated lncRNA NEAT1 stability in tumorigenesis and progression of ovarian cancer. Cancer Med. 2016; 5:1588–98. [PubMed: 27075229]
18. Abdelmohsen K, Gorospe M. Posttranscriptional regulation of cancer traits by HuR. Wiley Interdiscip Rev RNA. 2010; 1:214–29. [PubMed: 21935886]
19. Kakuguchi W, Kitamura T, Kuroshima T, Ishikawa M, Kitagawa Y, Totsuka Y, et al. HuR knockdown changes the oncogenic potential of oral cancer cells. Mol Cancer Res. 2010; 8:520–8. [PubMed: 20332213]
20. Babu, A., Amreddy, N., Muralidharan, R., Munshi, A., Ramesh, R. Nano Based Drug Delivery. J. Naik, IAPC Publishing; Croatia: 2015. Nanoparticle-mediated siRNA delivery for lung cancer treatment; p. 195-205.
21. Van der Giessen K, Di-Marco S, Clair E, Gallouzi IE. RNAi-mediated HuR depletion leads to the inhibition of muscle cell differentiation. J Biol Chem. 2003; 278:47119–28. [PubMed: 12944397]
22. Narsireddy A, Vijayashree K, Irudayaraj J, Manorama SV, Rao NM. Targeted in vivo photodynamic therapy with epidermal growth factor receptor-specific peptide linked nanoparticles. Int J Pharm. 2014; 471:421–9. [PubMed: 24939618]
23. Brigger I, Dubernet C, Couvreur P. Nanoparticles in cancer therapy and diagnosis. Adv Drug Deliv Rev. 2002; 54:631–51. [PubMed: 12204596]
24. Brannon-Peppas L, Blanchette JO. Nanoparticle and targeted systems for cancer therapy. Adv Drug Deliv Rev. 2004; 56:1649–59. [PubMed: 15350294]
25. Narsireddy A, Vijayashree K, Adimoolam MG, Manorama SV, Rao NM. Photosensitizer and peptide-conjugated PAMAM dendrimer for targeted in vivo photodynamic therapy. Int J Nanomedicine. 2015; 10:6865–78. [PubMed: 26604753]
26. Navath RS, Menjoge AR, Wang B, Romero R, Kannan S, Kannan RM. Amino acid-functionalized dendrimers with heterobifunctional chemoselective peripheral groups for drug delivery applications. Biomacromolecules. 2010; 11:1544–63. [PubMed: 20415504]
27. Tekade RK, Kumar PV, Jain NK. Dendrimers in oncology: an expanding horizon. Chem Rev. 2009; 109:49–87. [PubMed: 19099452]
28. Madaan K, Kumar S, Poonia N, Lather V, Pandita D. Dendrimers in drug delivery and targeting: Drug-dendrimer interactions and toxicity issues. J Pharm Bioallied Sci. 2014; 6:139–50. [PubMed: 25035633]
29. Dufès C, Uchegbu IF, Schätzlein AG. Dendrimers in gene delivery. Adv Drug Deliv Rev. 2005; 57:2177–202. [PubMed: 16310284]
30. Leamon CP, Low PS. Folate-mediated targeting: from diagnostics to drug and gene delivery. Drug Discov Today. 2001; 6:44–51. [PubMed: 11165172]
31. Yellepeddi VK, Kumar A, Maher DM, Chauhan SC, Vangara KK, Palakurthi S. Biotinylated PAMAM dendrimers for intracellular delivery of cisplatin to ovarian cancer: role of SMVT. Anticancer Res. 2011; 3:897–906.
32. Ramesh R, Ito I, Gopalan B, Saito Y, Mhashilkar AM, Chada S. Ectopic production of MDA-7/IL-24 inhibits invasion and migration of human lung cancer cells. Mol Ther. 2004; 9:510–8. [PubMed: 15093181]
33. Amreddy N, Muralidharan R, Babu A, Mehta M, Johnson EV, Zhao YD, et al. Tumor-targeted and pH-controlled delivery of doxorubicin using gold nanorods for lung cancer therapy. Int J Nanomedicine. 2015; 10:6773–88. [PubMed: 26604751]
34. Akinc A, Thomas M, Klibanov AM, Langer R. Exploring polyethylenimine-mediated DNA transfection and the proton sponge hypothesis. J Gene Med. 2005; 7:657–63. [PubMed: 15543529]
35. Yellepeddi VK, Vangara KK, Palakurthi S. Poly(amido)amine (PAMAM) dendrimer–cisplatin complexes for chemotherapy of cisplatin-resistant ovarian cancer cells. J Nanopart Res. 2013; 15:1897–912.
36. Conti DS, Brewer D, Grashik J, Avasarala S, da Rocha SR. Poly(amidoamine) dendrimer nanocarriers and their aerosol formulations for siRNA delivery to the lung epithelium. Mol Pharm. 2014; 11:1808–22. [PubMed: 24811243]
37. Turner JJ, Jones SW, Moschos SA, Lindsay MA, Gait MJ. MALDI-TOF mass spectral analysis of siRNA degradation in serum confirms an RNAse A-like activity. Mol Biosyst. 2007; 3:43–50. [PubMed: 17216055]

38. Greenbaum D, Colangelo C, Williams K, Gerstein M. Comparing protein abundance and mRNA expression levels on a genomic scale. Genome Biol. 2003; 4:117. [PubMed: 12952525]

39. Muralidharan R, Babu A, Amreddy N, Srivastava A, Chen A, Zhao YD, et al. Tumor-targeted Nanoparticle Delivery of HuR siRNA inhibits lung tumor growth in vitro and in vivo by disrupting the oncogenic activity of the RNA-binding protein HuR. Mol Cancer Ther. 2017; 16:1470–86. [PubMed: 28572169]

40. Muralidharan R, Babu A, Amreddy N, Basalingappa K, Mehta M, Chen A, et al. Folate receptor-targeted nanoparticle delivery of HuR-RNAi suppresses lung cancer cell proliferation and migration. J Nanobiotechnology. 2016; 14:47. [PubMed: 27328938]

41. Haxton KJ, Burt HM. Hyperbranched polymers for controlled release of cisplatin. Dalton Trans. 2008:5872–5. [PubMed: 19082039]

42. Mehta M, Basalingappa K, Griffith JN, Andrade D, Babu A, Amreddy N, et al. HuR silencing elicits oxidative stress and DNA damage and sensitizes human triple-negative breast cancer cells to radiotherapy. Oncotarget. 2016; 7:64820–35. [PubMed: 27588488]

43. Muralidharan R, Mehta M, Ahmed R, Roy S, Xu L, Aubé J, et al. HuR-targeted small molecule inhibitor exhibits cytotoxicity towards human lung cancer cells. Sci Rep. 2017; :7.doi: 10.1038/s41598-017-07787-4 [PubMed: 28127057]

44. Blanco FF, Preet R, Aguado A, Vishwakarma V, Stevens LE, Vyas A, et al. Impact of HuR inhibition by the small molecule MS-444 on colorectal cancer cell tumorigenesis. Oncotarget. 2016; doi: 10.18632/oncotarget.12189

45. Romeo C, Weber MC, Zarei M, DeCicco D, Chand SN, Lobo AD, et al. HuR contributes to TRAIL resistance by restricting death receptor 4 expression in pancreatic cancer cells. Mol Cancer Res. 2016; 14:599–611. [PubMed: 27053682]

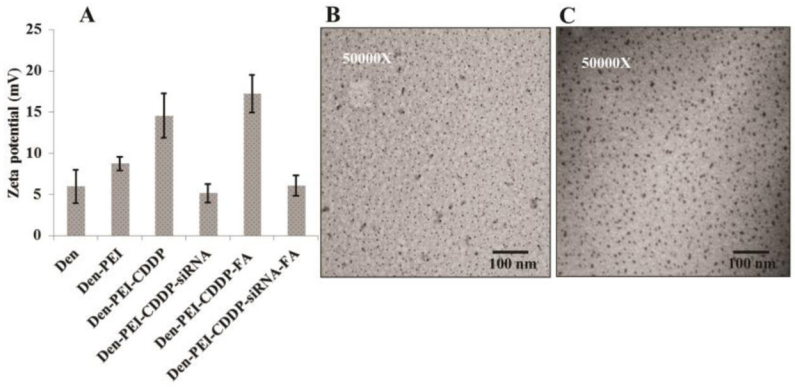

Figure 1.

Characterization of Den-PEI-CDDP-siRNA-FA nanoparticles. **(A)** Surface charge measurement by zeta potential each step of nanoparticle modification to form Den-PEI-CDDP-siRNA-FA. (n=5) **(B and C)** TEM images of Den-PEI and Den-PEI-CDDP-siRNA-FA nanoparticles.

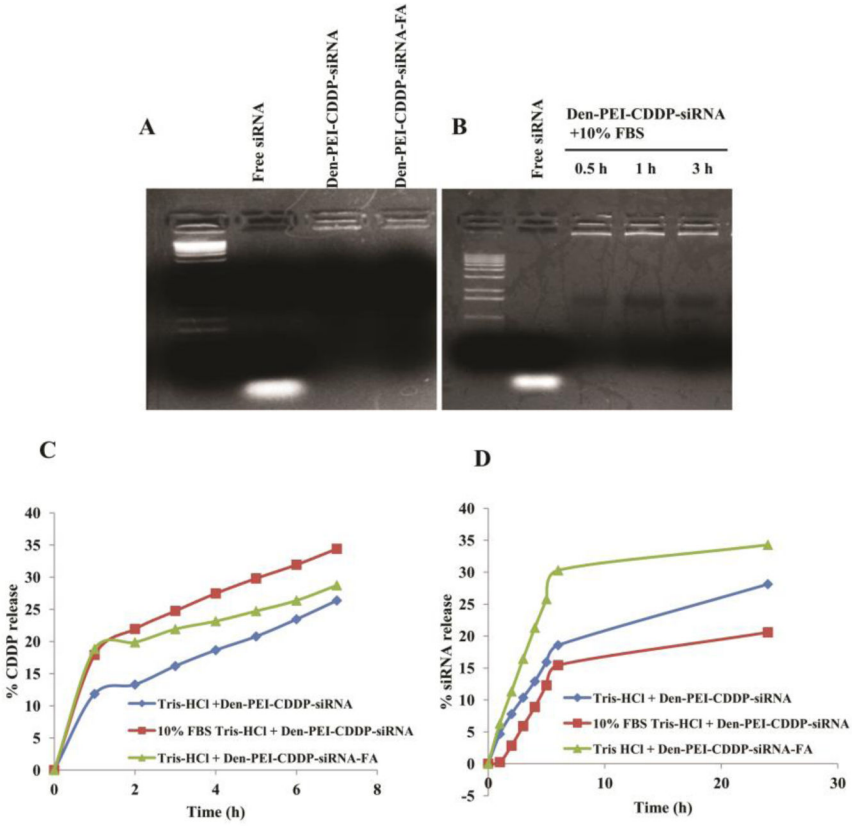

Figure 2.

Gel retardation assays and *in vitro* drug/siRNA release profiles of Den-PEI-CDDP-siRNA-FA. **(A)** siRNA encapsulation study of agarose gel with free siRNA, 10:1 N/P ratio of Den-PEI-CDDP-siRNA and Den-PEI-CDDP-siRNA-FA. **(B)** Agarose gel electrophoretogram showing siRNA protection efficiency of Den-PEI-CDDP-siRNA nanoparticles incubated in 10% FBS at 30 min, 1 h, and 3 h, respectively, compared with free siRNA. **(C and D)** *In vitro* CDDP and siRNA release profiles from Den-PEI-CDDP-siRNA nanoparticles in the presence and absence of 10% FBS in Tris-HCl buffer (pH 7.4) and Den-PEI-CDDP-siRNA-FA nanoparticles in Tris-HCl buffer (pH 7.4).

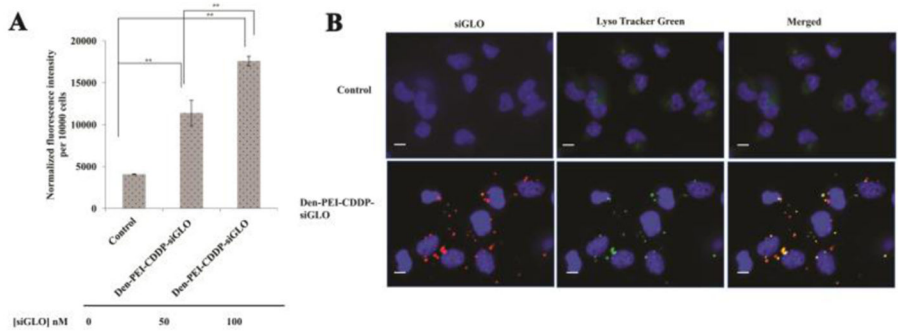

Figure 3.

Cell uptake study of Den-PEI-CDDP-siGLO nanoparticles in H1299 cells **(A)** Fluorescence intensity measurement of Den-PEI-CDDP-siGLO nanoparticles when incubated with H1299 cells for 24 h. (n=3) **(B)** Fluorescence microscopy images show the endosomal entrapment and escape of Den-PEI-CDDP-siGLO nanoparticles vs untreated control in H1299 cells. The Den-PEI-CDDP-siGLO was incubated with H1299 cells for 24 h, followed by LysoTracker Green staining and fluorescence microscopy. Images were taken at 60X magnification; (scale bar = 10μm, p ** <0.01).

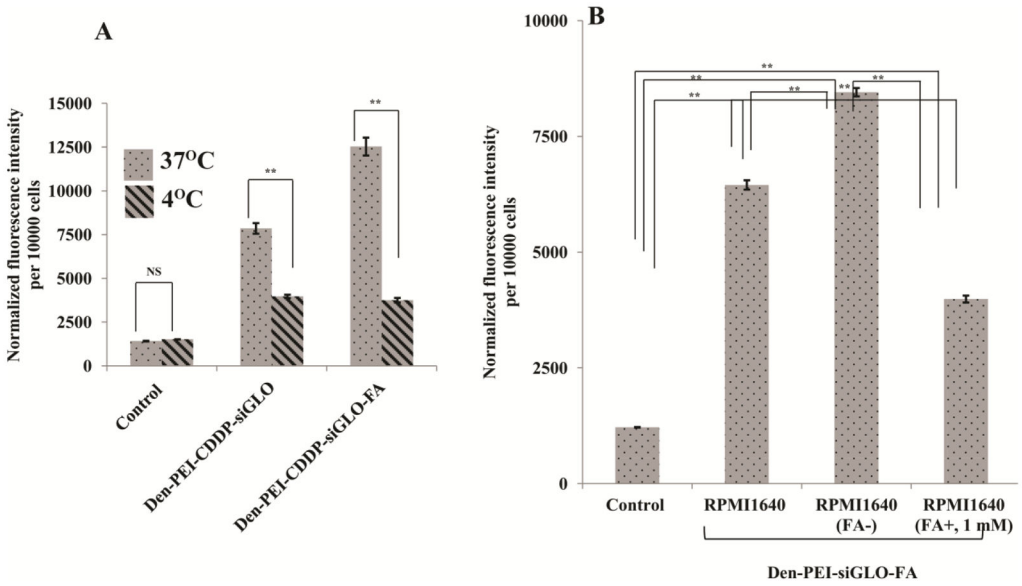

Figure 4.

FRA-mediated endocytosis study by fluorescence measurement in H1299 cells. **(A)** Temperature-dependent uptake of Den-PEI-CDDP-siGLO and Den-PEI-CDDP-siGLO-FA nanoparticles at 37°C and 4°C when incubated for 4 h, and **(B)** uptake of Den-PEI-siGLO-FA nanoparticles in H1299 cells when incubated for 24 h in RPMI-1640 medium containing endogenous levels of FA, without FA, or an excess of FA (1 mM). (n=3; ** denotes $p<0.01$, NS = not significant).

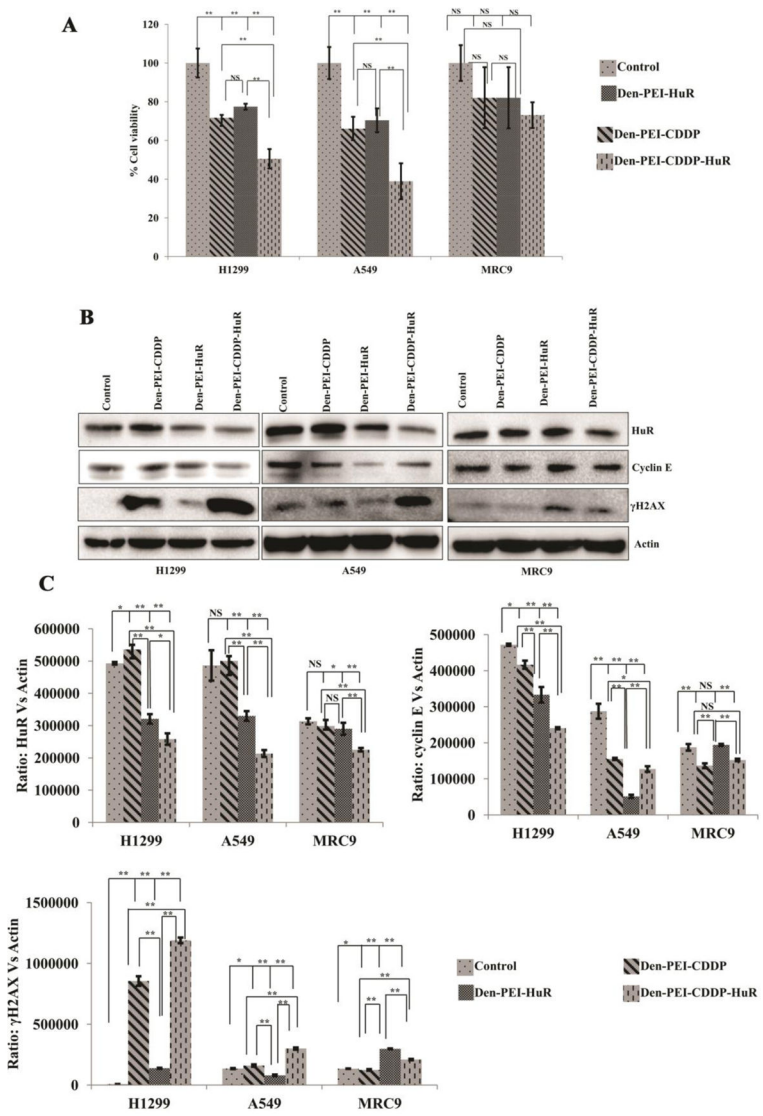

Figure 5.

The combined therapeutic efficacy of Den-PEI-CDDP-HuR nanoparticles compared with Den-PEI-CDDP and Den-PEI-HuR nanoparticles in H1299, A549, and MRC9 cells at 72 h. (**A**) Cell viability (n=4) and **(B)** western blot images of HuR, and cyclin E and γH2AX expression levels. **(C)** The respective band quantification values, in H1299, A549, and MRC9 cells. (** denotes $p < 0.01$, * denotes $p < 0.05$, NS = not significant).

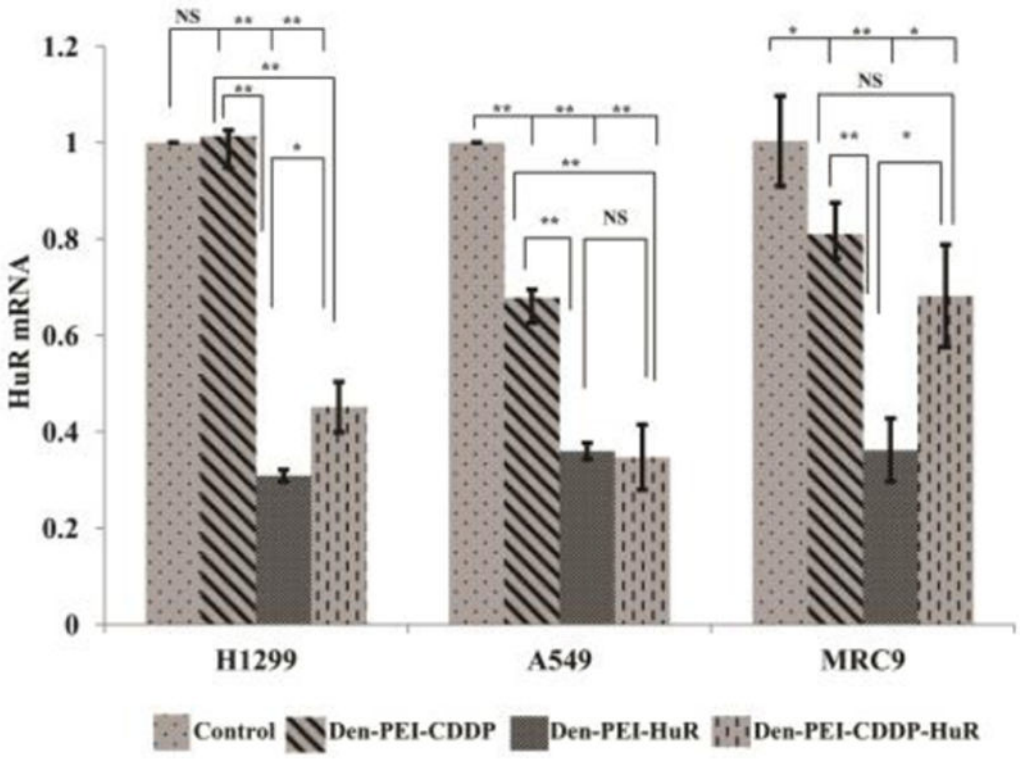

Figure 6.

HuR mRNA knockdown study by qRT-PCR. HuR mRNA knockdown analysis of Den-PEI-CDDP-HuR, Den-PEI-HuR, and Den-PEI-CDDP nanoparticles in H1299, A549, and MRC9 cells at 72 h. (n=3; ** denotes $p < 0.01$, *denotes $p < 0.05$, NS = not significant).

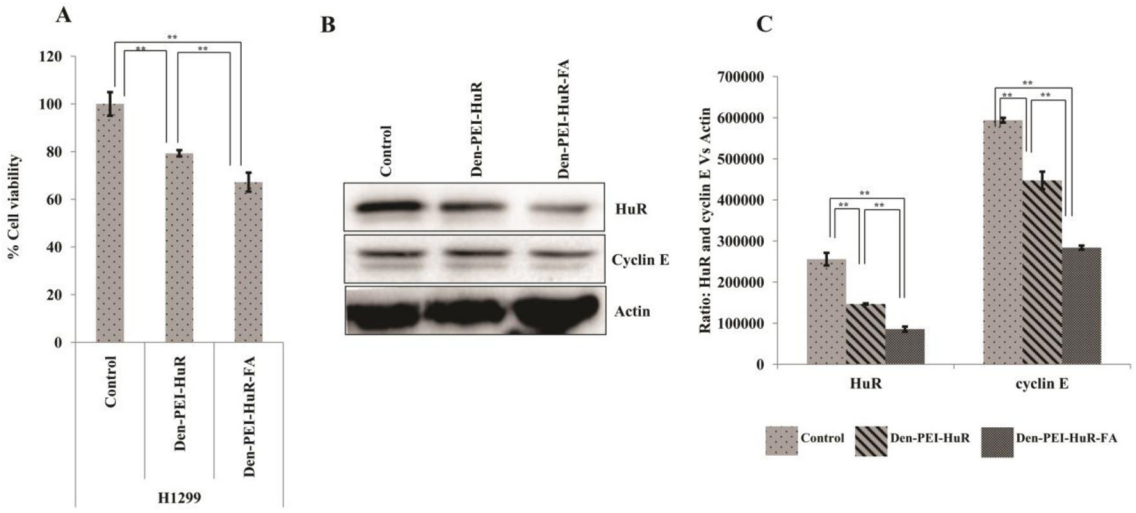

Figure 7.

Therapeutic efficiency of Den-PEI-HuR versus Den-PEI-HuR-FA in H1299 cells. **(A)** Cell viability and **(B & C)** western blot and respective band quantification graphs of HuR, cyclin E, and the internal control actin. (n=4; **denotes p <0.01, *denotes p <0.05, NS = not significant).

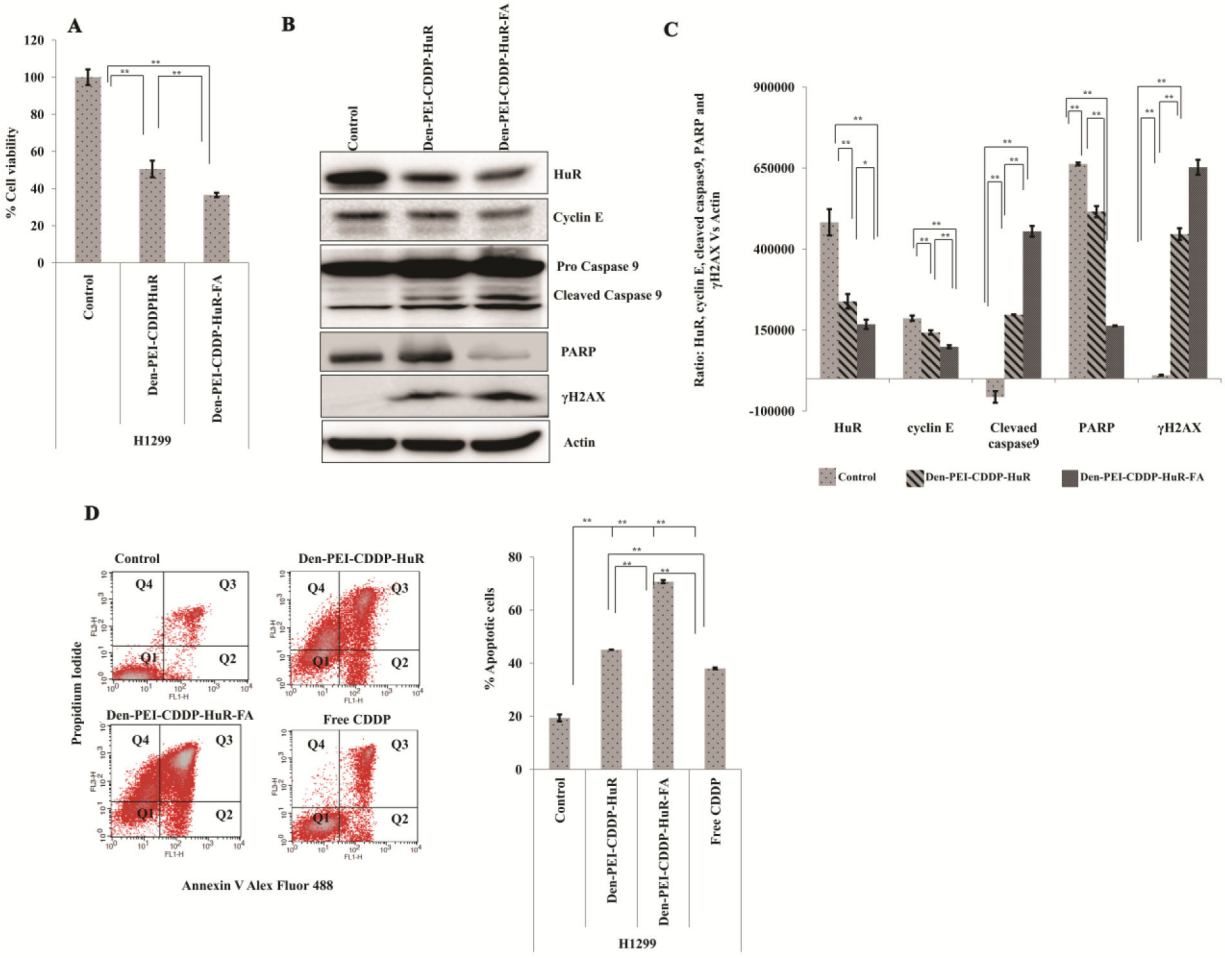

Figure 8.

Therapeutic efficiency of Den-PEI-CDDP-HuR versus Den-PEI-CDDP-HuR-FA in H1299 cells. **(A)** Cell viability assay, (n=4) **(B)** western blot analysis, and respective band (**C**) quantification graphs of HuR, cyclin E, cleaved caspase9, PARP, and γH2AX markers. **(D)** Dot plots showing distribution of cell population for analysis of apoptosis profile and the graphical representation of total apoptotic cell population (%) in H1299 cells when treated with Den-PEI-CDDP-HuR, Den-PEI-CDDP-HuR-FA, and free CDDP. Cells were dual stained with Alexa Fluor 488-Annexin V and propidium iodide after 72 h of treatment and were analyzed using flow cytometry (** denotes $p<0.01$, * denotes $p<0.05$, NS = not significant). (n=2; Q1, Annexin V and PI negative; Q2, Annexin V positive; Q3, Annexin V and PI positive; Q4, PI positive)

Table 1

CDDP and siRNA encapsulation efficiencies in Den-PEI and Den-PEI-FA nanoparticles

Nanoparticle	% CDDP encapsulation efficiency ± SD	% siRNA encapsulation efficiency ± SD
Den-PEI	35.65 ± 5.65	97.84 ± 0.12
Den-PEI-FA	40.52 ± 4.18	97.87 ± 0.10